Theoretical Study of Solid/Solid Interfaces in All-solid-state Batteries

Abstract

All-solid-state batteries (ASSBs) are widely investigated as promising energy storage systems with potentially high safety and design flexibility. The main problems to be overcome to bring ASSBs in real application are low conductivity at electrode/electrolyte interfaces as well as energy density. These problems can be solved by using high-energy-density cathodes with high stability. Ni-rich $LiNi_xCo_yMn_zO_2$ (NCM) cathodes doped with metals are promising candidates for these purposes. In the proposed project, we aim to find appropriate doping metal (*Me*) species that can improve the surface stability of $LiNi_{0.8}Co_{0.1}Mn_{0.1}O_2$ (NCM811) using quantum mechanics calculations. Moreover, we aim to evaluate stability of *Me*-doped NCM811 in contact with solid electrolytes. Here, we will focus on the most-commonly studied solid electrolyte material, namely $Li_7La_3Zr_2O_{12}$ (LLZO). Last year, we studied cation interchange between a coating Al_2O_3 layer and solid electrolyte $Li_{1.3}Al_{0.3}Ti_{1.7}(PO_4)_3$ (LATP) material, Li ion diffusion in *Me*-doped LLZO, and the effect of different types of doping on the properties of Ni-rich NMC (modelled by $LiNiO_2$) cathodes. In this proposed project, we aim to continue our study on finding the relation between the type of dopant and surface energy (mechanical stability) of NMC811 cathodes as well as cation interchange (i.e. stability) at NMC811/LLZO interfaces.

1. Organizational details

Title of the project:
Theoretical Study of Solid/Solid Interfaces in All-solid-state Batteries

Project leaders:

Dr. Payam Kaghazchi
Institut für Energie und Klimaforschung IEK-1: Werkstoffsynthese und Herstellungsverfahren
Forschungszentrum Jülich GmbH
D-52425 Jülich
payam.kaghazchi@fu-berlin.de

Project administrator:

Marvin Kosin
Institut für Energie und Klimaforschung IEK-1: Werkstoffsynthese und Herstellungsverfahren
Forschungszentrum Jülich GmbH
D-52425 Jülich
m.kosin@fz-juelich.de

2. Introduction

An important contribution to decreasing our dependency on fossil fuels is the development of electrochemical energy storage technologies, in particular Li-ion and all solid-state batteries (ASSBs). ASSBs hold the promise of overcoming the current constraints of conventional battery technologies such as limited long-term-stability and safety and are currently regarded as the next, revolutionary step in electrochemical energy storage. However, achieving the targets of high-capacity and high-performance solid-state batteries poses significant challenges and requires rational design of all components to increase capacity and minimize resistances. Among the fabricated cathode materials for Li-ion batteries, $LiNi_xCo_yMn_zO_2$ (NCM) is a promising cathode material because of its high theoretical capacity [1-5]. Higher Ni content in NCM cathodes leads to higher reversible capacity (*e.g.* 227 $mAhg^{-1}$ for $LiNi_{0.9}Co_{0.05}Mn_{0.05}O_2$ [6]). Ni-enriched NMC cathodes, however, suffer from capacity fading and thermal runaway problems [7,8]. Doping and substitution are promising strategies to improve the performance of Ni-rich NMC in terms of conductivity and stability [9-14]. Theoretical *ab initio* calculations have been applied to study the occupation site, mechanism of charge compensation, and solubility of several types of dopants as well as effect of types of several dopants on electronic and ionic conductivity, volume change, and stability of battery materials (for example please see refs. [15-22]). There are, however, only few studies on the possibility of segregation of dopant to the surface. For example, very recently Hou *et al.* [22] have investigated bulk and surface of Sn-doped $LiFePO_4$ and found that surface doping is energetically more favorable than bulk or subsurface doping leading to creation of Li vacancies and decrease in band gap. Most of ASSB systems show poor performance in practice mainly due to the large resistances, particularly at the electrolyte/electrode interfaces. Popular explanations for the high interfacial resistance are: (i) insulating new phases which are formed at the interfaces during cosintering at high temperatures [23,24] and/or charge/discharge process [25] and (ii) formation of space charge layers with lower ionic conductivity than bulk electrode or electrolyte [26-31].

Although last year, we proposed to work on the new phases that are formed during high-temperature processing at LLZO/LCO interfaces, but the composition of these phases was not characterized by experimental measurements due to the complexity of performing experiment on this interface. Thus, instead, we worked together with other experimentalist groups to find an appropriate coating layer between solid electrolyte and electrode to prevent new phase formation. Motivated by the results of our experimental collaborator, we investigated stability of an Al_2O_3 coating phase and solid LATP electrolyte with a Li electrode as well as cation interchange between Al_2O_3 and LATP [33]. The results will be summarized in the next subsection. Moreover, motivated by experimental result of our experimentalist partner at our institute, we calculated Li ion diffusion in c-LLZO, Ta-LLZO, and Al-LLZO. In addition, in our previous projects supported by HLRN, from 2017 to now, we have studied the effect of Zr- [34], W- [35], and B-doping [36] on LNO as well as Fe in $NaMnO_2$ cathode materials [37]. We determined the mechanism of charge compensation and lattice parameter change for Zr-doped LNO [34] as well as surface structure and stability for W-doped LNO [35]. In the next subsection, we will summarize our last year study on the effect of B doping on LNO [36] and Fe doping on $NaMnO_2$. The first work showed that B enhances the stability of (0001) surface in comparison to (10-14) which can result in large areas of (0001) facets in the particles of the boron-doped LNO cathodes. Regarding the Fe-doped $NaMnO_2$ project [37], for the first time, we have explained the relation between JT distortion and lattice parameter change. These results show that doping and substitution can affect performance of cathode materials. A systematic study of effect of dopant type on chemical and mechanical stability of cathode materials in absence and presence of solid electrolytes is still missing. These studies will be the subjects of the present proposal.

In the following, we summarize our obtained results **from 01.07.2018 to 27.04.2019** and then in the next section we discuss our strategy to continue this project.

WP. 1 To study the stability of solid LATP electrolyte and the coating α-Al_2O_3 layer in contact with a Li metal electrode, we have calculated absorption energies of a single Li atom in LATP and α-Al_2O_3, respectively, using DFT-PBE calculations. Our results show that the absorption energy of a single Li inside LATP is a large negative value of −2.88 eV, confirming the instability of LATP with respect to Li metal. However, the absorption energy of single Li in α-Al_2O_3 possesses a large positive value of +3.17 eV, providing an evidence for the high stability of this coating layer against Li metal (see Fig. 1). Moreover, we have studied the possibility of Al ↔ Ti interchange between LATP and α-Al_2O_3 following the procedure presented in Fig. 1. It is found that the interchange is unfavorable from a thermodynamic point of view because it requires 3.22 eV energy. We published the results of this work in ACS Applied Materials & Interfaces [33].

Together with our experimentalist collaborator, we are now studying diffusion coefficients, *D*, in pristine c-LLZO, Al-doped LLZO, and Ta-doped LLZO. We performed AIMD-NVT calculation for > 35 ps at five different temperatures. The calculated values of *D* were plotted as function of 1/*T* in Fig. 2. Our calculations clearly show that Al dopant blocks Li ion migration, but Ta dopant enhances the Li migration. We are now working together with experimentalist to analyze our data.

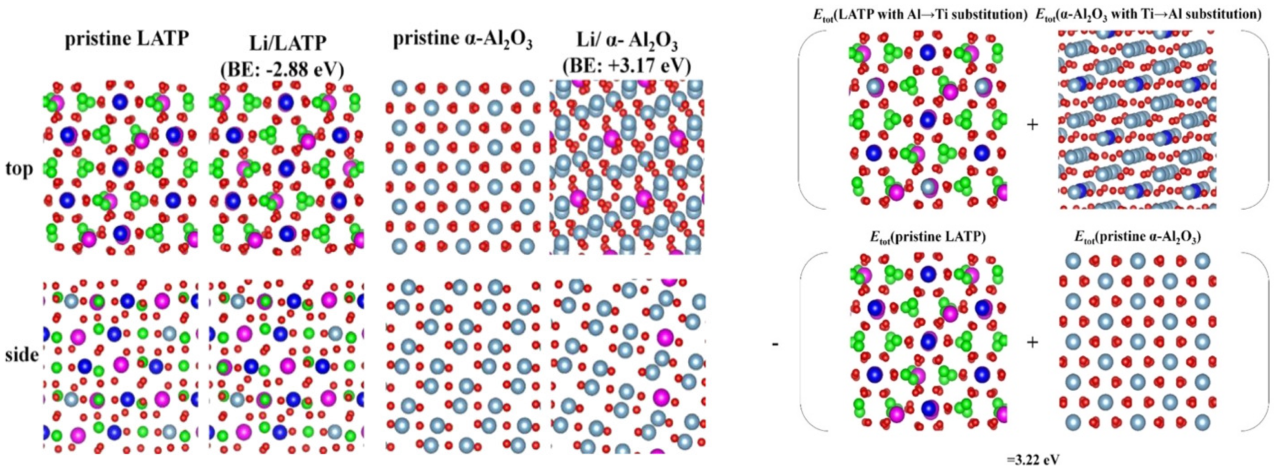

Fig. 1 (left panel) Calculated binding energies of a single Li into bulk LATP and α-Al_2O_3 is presented by BE. The BE values are referenced to bulk Li metal. (right panel) Schematic of the procedure to calculate the Al ↔ Ti interchange energy between LATP and α-Al_2O_3.

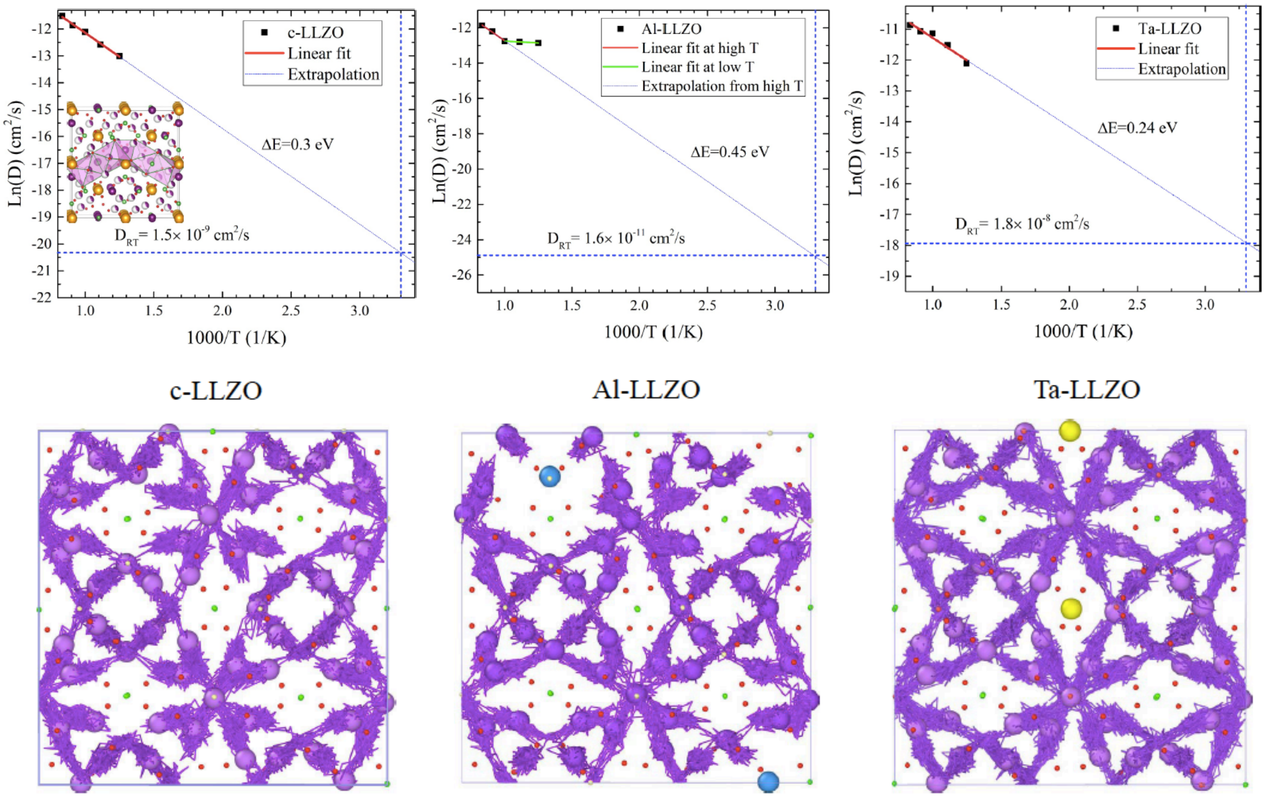

Fig. 2 Calculated Ln*D* for Li diffusion in c-LLZO, Al-LLZO, and Ta-LLZO as function of 1000/*T* (top panel) and corresponding integrated visited positions by Li ions at the whole AIMD run (bottom panel).

WP2. As mentioned above, due to the lack of understanding the composition of new phases, during the last-year project, we focused on Li ion diffusion in c-LLZO, Al-doped LLZO, and Ta-doped LLZO electrolyte as well as Li/α-Al_2O_3, Li/LATP, and α-Al_2O_3/LATP interfaces. Besides evaluation of the Li absorption energy in bulk α-Al_2O_3 and LATP as well as cation interchange energy between bulk α-Al_2O_3 and LATP, we performed DFT and AIMD simulations on explicit Li/α-Al_2O_3 and Li/LATP interfaces (see Fig. 3). We carried out an extensive DFT calculations to find the most favorable structures of the interfaces. Afterwards, we performed AIMD simulations. DFT calculation (at *T*=0 K) predicts that surfaces remain crystalline after geometry optimization. However, AIMD simulations at room temperature predict that α-Al_2O_3 is stable, but LATB becomes amorphous in contact with a Li metal surface. These results show that how AIMD simulations can be applied to investigate the stability of coating layers and electrolyte in contact with electrodes.

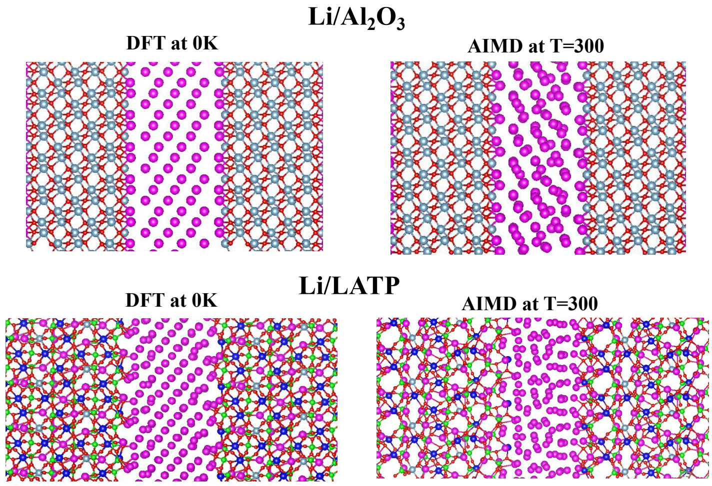

Fig. 3 Atomic structures of Li/α-Al_2O_3 and Li/LATP interfaces calculated using DFT and AIMD simulations at 0 K and 300 K.

WP3. We studied effect of B-doping on LNO as well as Fe doping on $Na_{2/3}MnO_2$. The reason that we chose $Na_{2/3}MnO_2$ was that we received a collaboration request from our experimentalist partner to study effect of doping on chemical and physical properties of Na-based cathodes. We also completed our year-before-last work on Zr- and W-doping of LNO and published the corresponding manuscripts in 2018 [34,35]. Last year, we studied effect of B on LNO [36] and found (see Fig. 4) that B enhances the stability of (0001) surface in comparison to (10-14) which can result in large areas of (0001) facets in the particles of the boron-doped LNO cathodes. Our experimentalist partners have further found that in the B-doped LNO particles internal strain involved with Li extraction/re-insertion decreases which leads to improved cycling stability. We applied a combined Coulomb energy analysis and DFT calculation to find the most-favorable structures of $Na_{2/3}Fe_xMn_{1-x}O_2$ with different Fe-dopant concentrations [37]. The most favorable structures for non-doped and Fe-doped $Na_{2/3}MnO_2$ are presented in Fig. 5. DFT calculations, in agreement with the experimental measurements, show that the lattice dimension *a* increases, while *b*, *c*, and J-T distortion decrease. Our analysis on O–Mn–O and O–Fe–O bond lengths for the case of 22% Fe doping explains this behavior. Fe dopants suppress the J-T distortion by increasing equatorial O–Me–O distances and decreasing axial O–Me–O ones. The equatorial O–Me–O length is exactly along the lattice vector *a*, which is perpendicular to *b* and *c* lattice vectors. Therefore, the Fe-doping-induced increase in the equatorial O–Me–O distances causes the lattice parameter *a* to expand. On the other hand, the axial O–Me–O bond is parallel to the *bc* plane. Thus, the Fe-doping-induced decrease in the axial O–Me–O length leads to the decrease in the lattice parameters *b* and *c*. Finally, Fe-doped decrease of JT distortion confirms higher stability of $Na_{2/3}FexMn_{1-x}O_2$ in comparison to $Na_{2/3}Mn_1O_2$.

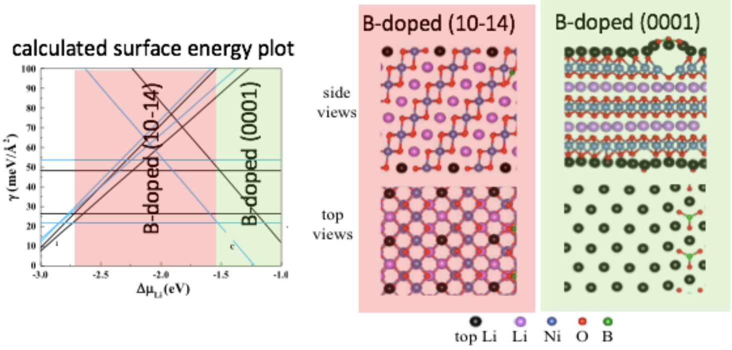

Fig. 4 Surface energy plot for B-doped (10-14) and (0001) surfaces (left panel). Atomic structures of B-doped (10-14) and (0001) surfaces (right panel).

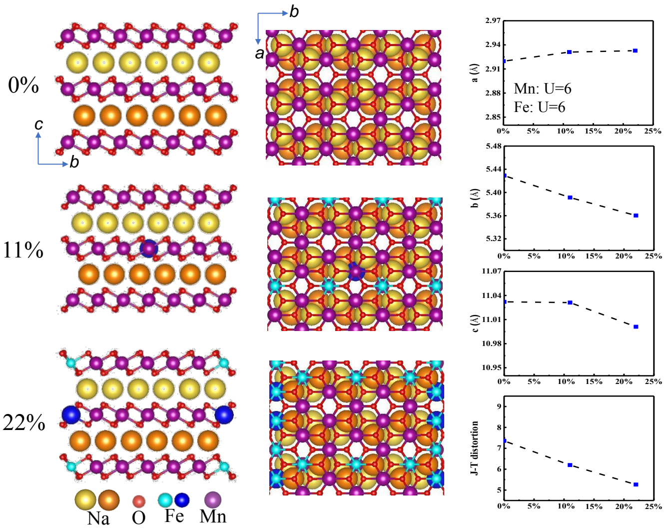

Fig. 5 Atomic structures and change in lattice parameters and J-T distortions of $Na_{2/3}MnO_2$ with different Fe dopant concentrations.

3. Project description and computational details

In the continuation of this project, we aim to focus on other types of dopants and find appropriate dopant types that can enhance mechanical and chemical stability of $LiNi_{0.8}Mn_{0.1}Co_{0.1}O_2$ (NMC811) cathodes for Li-based battery applications. We will focus on three various *Me*-doped NMC811 cathodes, most likely Al-doped, Fe-doped, and Nb-doped NMC811. Our choices of dopant types depend on our experimental collaborators at FZJ that will synthesize and characterize the *Me*-doped NMC811 cathodes. We will study mechanical and chemical stability by calculating surface energies

(γ, see eq. 1) and cation interchange energies ($E_{\mathrm{I}}^{\mathrm{x}\leftrightarrow\mathrm{y}}$, see eq. 2). The first quantity γ determines energy associated with a crack formation. The second one controls cation interchange between cathode and electrolyte. An important question is whether dopant segregate to the top layers or not, and if the segregation occurs how it can influence the surface energies of NMC surfaces. To estimate γ, we will use the following equation

$$\gamma = \frac{1}{2A}\left[E_{\mathrm{surf}} - E_{\mathrm{Bulk}} \pm \textstyle\sum_{i} N_{\mathrm{i}}\mu_{\mathrm{i}}\right], \tag{1}$$

where E_{surf} and E_{Bulk} are the total energy of surface and bulk structure, respectively. N_{i} and μ_{i} are number and chemical potential of the species in shortage (+) or excess (-). *A* is the surface area. This equation can be used for stoichiometric and nonstoichiometric with any termination. We will use Perdew-Burke-Ernzerhof (PBE) [38] + Hubbard U parameter exchange- correlation functional [39]. To calculate structures and energies of *Me*-doped bulk NMC we will focus on a concentration of about 2 percent dopant (with respect to Li concentration in NMC811) by using a 4×4×1 supercell and a single dopant (1 *Me*/48 Li). We will first optimize unit cell parameters and geometry of bulk NMC811 without and with dopants. To model surfaces we will use slabs with width of larger 14 Å and introduce a vacuum space of 12 Å between slabs. We will keep fixed the unit cell parameters as well as middle layers.

To calculate the interchange energy of cations between NMC811 and LLZO we will use the following equation

$$E_{\mathrm{I}}^{\mathrm{x}\leftrightarrow\mathrm{y}} = E_{\mathrm{NMC811}}^{\mathrm{x}\rightarrow\mathrm{y}} + E_{\mathrm{LLZO}}^{\mathrm{y}\rightarrow\mathrm{x}} - (E_{\mathrm{NMC811}}^{\mathrm{pristine}} + E_{\mathrm{LLZO}}^{\mathrm{pristine}}). \tag{2}$$

Here, $E_{\mathrm{NMC811}}^{\mathrm{x}\rightarrow\mathrm{y}}$ and $E_{\mathrm{LLZO}}^{\mathrm{y}\rightarrow\mathrm{x}}$ are total energies of bulk NMC811 with a substitution of x→y and LLZO with a substitution of y→x, respectively. $E_{\mathrm{NMC811}}^{\mathrm{pristine}}$ and $E_{\mathrm{LLZO}}^{\mathrm{pristine}}$ are total energies of pristine NMC811 and LLZO. To calculate $E_{\mathrm{I}}^{\mathrm{x}\leftrightarrow\mathrm{y}}$ we will use bulk model and focus on a concentration of 2 percent (with respect to Li concentration in NMC811) cation interchange. The same supercell as mentioned above (without vacuum) will be applied. Regarding LLZO, we will consider the conventional unit cell of *a* = 12:98 Å, *b* = 13:02 Å, and *c* = 13:02 Å with one substitution.

4. Work plan

WP1. Calculate surface structure and energy of *Me*-doped cathodes using electrostatic analysis, DFT calculation, and *ab initio* thermodynamics: We will study effect of dopant on the mechanical stability of NMC811 cathodes. To achieve this aim, we have to first find the most favorable structures of *Me*-doped NMC811 surfaces by calculating surface energies of possible orientations and terminations as well as dopant distribution. Previous theoretical studies, in agreement with experimental measurements have shown that (0001), (10-14), (11-20), and (01-12) surfaces are the most favorable facets of pristine NMC nanoparticles [40,41]. We will focus on these most probable surfaces and calculate energies (γ, see eq. 1) of the surfaces with various terminations (stoichiometric and nonstoichiometric) without and with dopant. We will consider both homogeneous (in bulk and top-most layers of slab) and non-homogeneous (in bulk or top-most layers of slab) distribution of dopants. This study will show possibility of segregation and its influence on surface energy and fracture formation.

WP2. Effect of dopant on the cation interchange between NMC811 and solid LLZO electrolyte: In this project, we will study effect of doping on the initial stage of new phase formation at the

NMC811/LLZO interface by calculating cation interchange energy, namely Ni↔Zr, Mn↔Zr, Co↔Zr, Ni↔La, Mn↔La, and Co↔La as well as dopant↔Zr and dopant↔La. To achieve this aim, we will follow the same approach as we introduced in our recently-published manuscript [33] using eq. 2.

5. Resource request

In our proposal for 2016-2017, we carried out geometry-optimization calculations for LLZO and LCO using different number of cores and processors and plotted speedup curves. Based on this curve and our recent calculations, I will give the details of the required number of core-hours for performing our project.

WP1. We will study stability of **3** *Me*-doped NMC811 surfaces (most likely Al-doped, Fe-doped, and Nb-doped NMC811). We will focus on **4** possible terminations of **4** surface orientations of (0001), (10-14), (11-20), and (01-12). We will consider **3** possible arrangements of dopants (in both bulk and surface, only bulk, and only surface region). We will calculate stability of **2** different Li contents of *Me*-doped NMC811, namely full and half occupancies. Based on our experience with W-doped LNO(0001) system, each DFT calculation needs 6912 core hours (about 576 NPL). Therefore, for **3** types of dopants, **4** surfaces with **4** various terminations, **3** dopant configurations, and **2** different Li contents we need 3*4*4*3*2*6912= 1990656 core hours (about 165888 NPL). Moreover, we need to compare our results to non-doped cases. We, therefore, need to model **4** surfaces with **4** various terminations, and **2** different Li contents: 4*4*2*6912=221184 core hours (about 18432 NPL).

WP2. To find the most favorable structures of cation-interchange between bulk NMC811 and LLZO we need to calculate total energies of the following structures: i) both **1** pristine and **3** *Me*-doped NMC811 with La→Ni, La→Mn, La→Co, and La→*Me* substitution (pristine: **3** sets, *Me*-doped: **4** sets) and ii) LLZO with Ni→La, Mn→La, Co→La, *Me*→La (**4** substitutions***24** La sites) as well as Ni→Zr, Mn→Zr, Co→Zr, and *Me*→Zr substitution (**4** substitutions***16** Zr sites). For the case of NMC811 we will consider full- and half-lithiated states (**2** sets). Based on our experience for pristine and *Me*-doped NMC811 and LLZO calculations, we need a similar value of core-hours to the calculation of WP1. Therefore we need ((1*3+3*4)*2)*6912+(4*24+4*16)*6912=1313280 core-hours (about 109440 NPL).

Milestones	required core hours	required NPL
WP1. Calculate surface free energies of pristine and Me-doped NMC using DFT calculations	2211840	184320
WP2. Modeling of space charge at LLZO/NMC	1313280	109440
Total required core hours or NPL for 1 year	3525120	293760

References

[1] J. R. Dahn, U. V. Sacken and C. A. Michal, Solid State Ionics, 1990, 44, 87.
[2] E. Rossen, C. D. W. Jones and J. R. Dahn, Solid State Ionics, 1992, 57, 311.
[3] C. Delmas, I. Saadoune and A. Rougier, J. Power Sources, 1993, 44, 595.
[4] Y.-K. Sun, S.-T. Myung, H.-S. Shin, Y. C. Bae and C. S. Yoon, J. Phys. Chem. B, 2006, 110, 6810.
[5] L. Biasi, A. O. Kondrakov, H. Geßwein, T. Brezesinski, P. Hartmann and J. Janek, J. Phys. Chem. C, 2017, 121, 26163.
[6] C. Yoon, M. Choi, B.-B. Lim, E.-J. Lee and Y.-K. Sun, J. Electrochem. Soc., 2015, 162, A2483.
[7] H.-H. Ryu, K.-J. Park, C. Yoon and Y.-K. Sun, Chem. Mater., 2018, 30, 1155.
[8] S.-M. Bak, E. Hu, Y. Zhou, X. Yu, S. D. Senanayake, S.-J. Cho, K.-B. Kim, K. Chung, X.-Q. Yang and K.-W. Nam, ACS Appl. Mater. Interfaces, 2014, 6, 22594.
[9] H. Buschmann, J. Dölle, S. Berendts, A. Kuhn, P. Bottke, M. Wilkening, P. Heitjans, A. Senyshyn, H. Ehrenberg, A. Lotnyk, V. Duppel, L. Kienlee and J. Janek, Phys. Chem. Chem. Phys., 2011, 13, 19378.
[10] H. E. Shinawi and J. Janek, J. Power Sources, 2013, 225, 13.
[11] M. Matsui, K. Takahashi, K. Sakamoto, A. Hirano, Y. Takeda, O. Yamamoto and N. Imanishi, Dalton Trans., 2014, 43, 1019.
[12] H. Tukamoto and A. R. West, J. Electrochem. Soc. 1997, 144, 3164.
[13] A. Rougier, I. Saadoune, P. Gravereau, P. Willmann and C. Delmasa, Solid State Ionics 1996, 90, 83.
[14] C. S. Yoon, M.-J. Choi, D.-W. Jun, Q. Zhang, P. Kaghazchi, K.-H. Kim and Y.-K. Sun, Chem. Mater. 2018, 30, 1808.
[15] Koyama, Y.; Arai, H.; Tanaka, I.; Uchimotoc, Y.; Ogumi, Z., J. Mater. Chem. A 2014, 2, 11235.
[16] Kim, S.; Choi, S.; Lee, K.; Yang, G. J.; Lee, S. S.; Kim, Y., Self-assembly of core-shell structures driven by low doping limit of Ti in $LiCoO_2$: first-principles thermodynamic and experimental investigation. Phys. Chem. Chem. Phys. 2017, 19, 4104.
[17] Hoang, K., First-principles theory of doping in layered oxide electrode materials. PHYSICAL REVIEW MATERIALS 2017, 1, 075403.
[18] Shi, S.; Ouyang, C.; Lei, M.; Tang, W., Effect of Mg-doping on the structural and electronic properties of $LiCoO_2$: A first-principles investigation. Journal of Power Sources 2007, 171, 908.
[19] Ning, F.; Xu, B.; Shi, J.; Wu, M.; Hu, Y.; Ouyang, C., J. Phys. Chem. C 2016, 120, 18428.
[20] Haoa, S.; Zhaoa, N.; Shia, C.; Hea, C.; Lia, J.; Liu, E., Ceramics International 2015, 41, 2294.
[21] Chen, H.; Dawson, J. A.; Harding, J. H., J. Mater. Chem. A 2014, 2, 7988.
[22] Hou, L.; Tao, G., Phys. Status Solidi B 2017, 254, 1700041.
[23] Miara, L.; Windmüller, A.; Tsai, C.-L.; Richards, W. D.; Ma, Q.; Uhlenbruck, S.; Guillon, O.; Ceder, G., ACS Appl. Mater. Interfaces 2016, 8, 26842.
[24] Kim, K. H.; Iriyama, Y.; Yamamoto, K.; Kumazaki, S.; Asaka, T.; Tanabe, K.; Fisher, C. A. J.; Hirayama, T.; Murugan, R.; Ogumi, Z., J. Power Sources 2011, 196, 764.
[25] Sakuda, A.; Hayashi, A.; Tatsumisago, M., Chem. Mater. 2010, 22, 949.
[26] Ohta, N.; Takada, K.; Zhang, L.; Ma, R.; Osada, M.; Sasaki, T., Adv. Mater. 2006, 18, 2226.
[27] Schichtel, P.; Geiß, M.; Leichtweiß, T.; Sann, J.; Weber, D. A.; Janek, J., J. Power Sources 2017, 360, 593.
[28] Maier, J., Phys. Chem. 1985, 89, 355.
[29] Bazant, M. Z.; Chu, K. T.; Bayly, B. J., J. Appl. Math. 2005, 65, 1463.
[30] Landstorfer, M.; Funken, S.; Jacob, T., Phys. Chem. Chem. Phys. 2011, 13, 12817.
[31] Luntz, A. C.; Voss, J.; Reuter, K., J. Phys. Chem. Lett. 2015, 6, 4599.
[32] S. Panahian Jand and P. Kaghazchi, MRS Communications 2018, 1-6.
[33] Y. Liu, Q. Sun, Y. Zhao, B. Wang, P. Kaghazchi, K. Adair, R. Li, R. Yang; S. Lu, X. Song, and X. Sun, ACS Applied Materials & Interfaces 2018, 10 (37), 31240.
[34] C. S. Yoon, Q. Zhang, P. Kaghazchi, and Y.-K. Sun, Chem. Mater. 2018, 30(5), 1808.
[35] U-H Kim, Q. Zhang, P. Kaghazchi, D. Aurbach, D. T. Major, G. Goobes, M. Dixit, P. Yan, D. Ahn, Kwang Ho Kim, Chong S. Yoon, Yang-Kook Sun, Energy Environ. Sci. 2018, 11, 1271.
[36] K-J Park, L-Y. Kuo, P. Kaghazchi, H-G Jung, C. S. Yoon, and Y-K Sun, Advanced Energy Materials 2018, 8 (25), 1801202.
[37] J. U. Choi, Y. J. Park, J. H. Jo, L-Y Kuo, P. Kaghazchi, and S-T Myung, ACS Appl. Mater. Interfaces

2018, 10(48), 40978.
[38] J. P. Perdew, K. Burke, and M. Ernzerhof, Phys. Rev. Lett. 1996, 77, 3865.
[39] S. L. Dudarev, G. A. Botton, S. Y. Savrasov, C. J. Humphreys, A. P. Sutton, Phys. Rev. B: Condens. Matter Mater. Phys. 1998, 57, 1505.
[40] J. C. Garcia, J. Bareño, J. Yan, G. Chen, A. Hauser, J. R. Croy, and H. Iddir, The Journal of Physical Chemistry C 2017, 121 (15), 8290.
[41] C. Liang, R. C. Longo, F. Kong, C. Zhang, Y. Nie, Y. Zheng, and K. Cho, ACS Applied Materials & Interfaces 2018, 10 (7), 6673.